UDC 331.45 https://doi.org/10.23947/2541-9129-2021-1-26-37

Theoretical study of the model of air flow movement near the shaped shelter of the rough grinding machine

I. S. Kuptsova
Don State Technical University (Rostov-on-Don, Russian Federation)

Introduction. The article deals with the problems of choosing equipment for effective dust removal and subsequent dust collection. The dependences describing the fields of flow velocities in the closed area of the abrasive wheel, influencing the formation of streamlines of flow motion near the shaped shelter of the rough grinding machine, are considered.
Problem Statement. The objective of this research is to develop a mathematical and computer model of the aspiration of a rough grinding machine.
Theoretical Part. To accomplish the set task, the modern software Ansys was used as well as the previously obtained results of the dispersion analysis of abrasive-cast iron dust during grinding, which had been carried out using a High-class device — an Analysette22 NanoTec laser granulometer.
Conclusion. The results of the analysis, the obtained fields and the values of the air flow velocities in the workplace of the machine operator will be compared with the hovering rates of various dust particles, which will allow us to determine the efficiency of the rough grinding machine shelter, including at the design stage.

Keywords: aspiration, Ansys, dust, peeling machine, computer model, mathematical model.

***For citation*:** Kuptsova I. S. Theoretical study of the model of air flow movement near the shaped shelter of the rough grinding machine: Safety of Technogenic and Natural Systems. 2021;1:26−37. https://doi.org/10.23947/2541-9129-2021-1-26-37

Introduction. To remove dry dust particles of different dispersion from under the shelters of technological equipment, aspiration with dust-collecting and dust-cleaning equipment is used, the efficiency of which is provided by a preliminary aerodynamic calculation.

Since the capture of dust particles in aspiration systems and dust cleaning devices is characterized by the competition of inertial and aerodynamic forces, the calculation is based on the physical criteria that make up the geometry of the particles with their mass.

To remove dust effectively and then collect it, it is necessary to develop:

— a mathematical model for the dispersion of abrasive-cast-iron dust during rough grinding of brittle parts;

— mathematical and computer models of aspiration of a rough grinding machine;

— to propose an engineering method for calculating the efficiency of the shaped shelter and selecting the elements of the dust removal and dust collection system for grinding machines of the class under consideration.

The mathematical and computer models of aspiration of a rough grinding machine, implemented in the modern software Apsus, are presented below.

The dependences describing the velocity fields of the flow movement in the closed area of the abrasive wheel are obtained, which influence the formation of flow lines near the shaped shelter of the rough grinding machine, which will further determine the efficiency of the shelter of the rough grinding machine, including at the design stage.

Problem Statement. In the process of roughing and grinding, two dust streams (plumes) are formed at the point of contact of the part and the abrasive wheel. The first stream moves tangentially to the circle of the abrasive wheel (straight plume), the other stream is directed along the rotation of the abrasive wheel itself (reverse plume) (Fig. 1). The shape and direction of these dust streams are visible on the firing lines formed during the operation of the grinding machine.

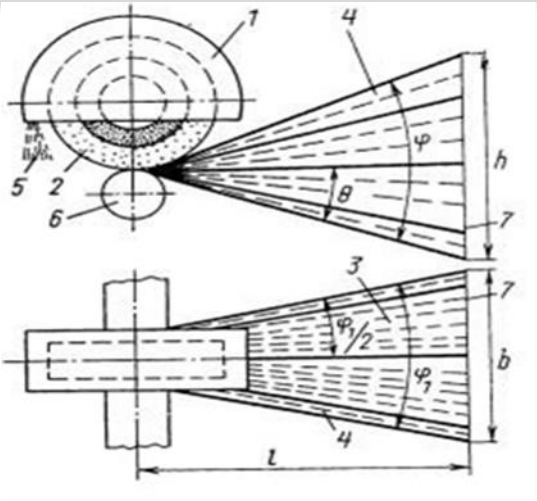

Fig. 1. Dust flows formed during grinding: 1 — cover, 2 — abrasive wheel, 3 — straight plume, 4 — invisible part of the plume, 5 — reverse plume, 6 — work piece, 7 — dust collector

When grinding without cooling the main stream of dust particles is wedge-shaped and directed in the direction of rotation of the abrasive wheel (Fig. 1). The wedge angle φ is the deviation of the main flow from the machined surface of the workpiece; it depends on the cutting parameters and physical and mechanical properties of the processed material [1].

The maximum efficiency of dust collection of abrasive-metal dust during grinding can be achieved if the design features of the dust collector are observed, taking into account the direction of movement of dust particles, as well as the possibility of regulating the design of the dust collector during the abrasive wheel wear. It is important that the dust collector is connected to the protective cover (casing) of the grinding machine. Shelters-dust collectors with storage devices are considered perfect if they require slightly less air for effective dust extraction due to the use of the kinetic energy of the flying chips and dust (Fig. 2) [2–3].

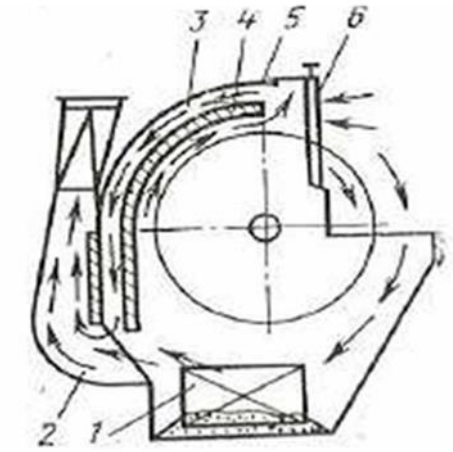

Fig. 2. The scheme of the fence of the dust collector for a grinding machine with a large dust accumulator: 1 — large dust accumulator, 2 — suction pipe, 3 — channel, 4 — partition, 5 — housing, 6 — flap to prevent dust from entering the workplace

The efficiency of dust collection and the safety of the grinding process largely depend on the design parameters of the protective casing-dust collector, including the size of the gap between the circle and the casing.

The protective casing must meet a number of requirements:

— the material for casing manufacture must have the maximum strength to prevent damage to the casing when the abrasive wheel breaks;

— the area of the cover of the abrasive wheel should be maximum, but not obstructing the processing of the part;

— the ability to adjust the position of the casing along the spindle axis, taking into account the wear of the wheel;

— the use of the casing as a dust intake, taking into account the direction of movement of dust flows;

— the possibility of attaching a dust-collecting device to the casing as the first stage of cleaning [2-3].

$$\frac{\partial \rho}{\partial t} + \frac{\partial}{\partial x_i}\left(\rho u_i\right) = 0, \tag{1}$$

where x_i —— the i-th spatial coordinate, m;

equation of moments (motion):

$$\frac{\partial(\rho u_i)}{\partial t} + \frac{\partial(\rho u_i i_j)}{\partial x_j} = -\frac{\partial p}{\partial x_i} + \frac{\partial}{\partial x_j}\left(\mu\left(\frac{\partial u_i}{\partial x_j} + \frac{\partial u_j}{\partial x_i}\right)\right) + G_i \tag{2}$$

Heat transfer is determined by the equation:

$$\frac{\partial(\rho h)}{\partial t} + \frac{\partial(\rho u_i h)}{\partial x_i} = \frac{\partial}{\partial x_i}\left(\mu \frac{\partial h}{\partial x_i}\right) + Q, \tag{3}$$

where Q —— the function of heat sources, W/m^3;

energy equation for the calculation of temperature characteristics:

$$\frac{\partial(\rho T)}{\partial t} + \frac{\partial(\rho u_i T)}{\partial x_i} = \frac{\partial}{c_p \cdot \partial x_i}\left(k \frac{\partial T}{\partial x_i}\right), \tag{4}$$

where ρ — density, P — pressure, u_i — components of the velocity vector, T — temperature, x_i — coordinates, μ — viscosity, c_p — specific heat capacity, k — thermal conductivity, $G_i = -\rho \cdot g_i$ — gravity component, h — enthalpy.

When using k-ω turbulence models, equations (1)–(2) are converted to form (4), in which the influence of the average velocity fluctuation (in the form of turbulent kinetic energy) and the process of reducing this fluctuation due to viscosity (dissipation) are added.

Two additional equations for the transport of the kinetic energy of turbulence and the equation for the rate of dissipation of the turbulent energy (5)–(6) are also added.

$$\frac{\partial(\rho k)}{\partial t} + \frac{\partial(\rho \bar{u}_i k)}{\partial x_j} = \frac{\partial}{\partial x_j}\left(\left(\mu + \frac{\mu_t}{\sigma_{k1}}\right)\frac{\partial k}{\partial x_j}\right) + P_k - \beta' \cdot \rho \cdot k \cdot \omega, \tag{5}$$

$$\frac{\partial(\rho \omega)}{\partial t} + \frac{\partial(\rho \bar{u}_j \omega)}{\partial x_j} = \frac{\partial}{\partial x_j}\left(\left(\mu + \frac{\mu_t}{\sigma_{k1}}\right)\frac{\partial \omega}{\partial x_j}\right) + \alpha_1 \cdot \frac{\omega}{k} \cdot P_k - \beta_1 \cdot \rho \cdot \omega^2, \tag{6}$$

k-equation:

$$\frac{\partial(\rho k)}{\partial t} + \frac{\partial(\rho u_j k)}{\partial x_j} = P_k - \rho \cdot C_\mu \cdot k \cdot \omega + \frac{\partial}{\partial x_j}\left(\left(\mu + \frac{\mu_t}{\tilde{\sigma}_k}\right)\frac{\partial k}{\partial x_j}\right), \tag{7}$$

ω-equation:

$$\frac{\partial(\rho\omega)}{\partial t}+\frac{\partial(\rho u_j\omega)}{\partial x_j}=\tilde{C}_{\omega 1}\frac{\omega}{k}\cdot P_k-\tilde{C}_{\omega 2}\cdot\rho\cdot\omega^2+(1-F)\cdot\frac{2\cdot\rho}{\sigma_\omega\cdot\omega}\cdot\frac{\partial k}{\partial x_j}\cdot\frac{\partial\omega}{\partial x_j}+$$
$$+\frac{\partial}{\partial x_j}\left(\left(\mu+\frac{\mu_t}{\tilde{\sigma}_\omega}\right)\frac{\partial\omega}{\partial x_j}\right), \quad (8)$$

where,

$$\tilde{\varphi}=\varphi_1\cdot F_1+\varphi_2\cdot(1-F_1), where \tilde{\varphi}=\tilde{C}_{\omega 1},\tilde{C}_{\omega 2},\frac{1}{\tilde{\sigma}_k},\frac{1}{\tilde{\sigma}_\omega},$$

$C_{\omega 11}=0,55; C_{\omega 21}=0,075; \sigma_{k1}=2; \sigma_{\omega 1}=2; C_\mu=0,09$

$C_{\omega 12}=0,44; C_{\omega 22}=0,083; \sigma_{k2}=1; \sigma_{\omega 2}=1,17$

μ_t — the coefficient of turbulent dynamic viscosity, k — turbulent kinetic energy (in the case of laminar flows k=0).

The boundary conditions for the system of equations (1)–(8) are the following parameters (Table 1).

Table1

Boundary conditions of the boundary value problem

Speed: u_i	(9)
Static exit pressure 0 relative to the external pressure (free boundary). P=0. All pressures here and below are set and obtained in the results relative to the external pressure. To obtain the total pressure, add the atmospheric pressure to these values.	(10)
On the inner walls, the adhesion conditions, the velocities are equal to 0.0. $u_i = 0$	(11)

For the energy equation (3)–(4), the boundary conditions are given in two versions. The heat flow on the walls q is determined from the formula:

$$q = h\cdot(T_1 - T_2), \quad (12)$$

where h — heat transfer coefficient, T_1 — temperature on the outer wall, T_2 — temperature on the inner wall.

The temperature on the outer wall T_1 and the heat transfer coefficient h. Further, the boundary value problem (3)–(12) can be solved numerically [4–13].

The equation of state for an ideal gas corresponds to the Mendeleev-Clapeyron law, the variable density can be calculated from the formula:

$$\rho=\frac{P\cdot M}{R\cdot T}, \quad (13)$$

where ρ — air density, P — pressure, R — gas constant, J/(mol·K), T — temperature, M — molecular weight of the air (28.966 g/mol).

The dependence of the viscosity coefficient on the thermodynamic values is established using the kinetic theory. In the calculations, the Sutherland formula is used to determine the dynamic viscosity coefficient:

$$\mu=\left(\frac{T}{273,15}\right)^{\frac{2}{3}}\cdot\frac{273,15+C_S}{T+C_S}\cdot\mu_0, \quad (14)$$

where C_s — Sutherland constant, μ_0 — the dynamic viscosity coefficient under normal conditions, kg/m s.

The initial conditions for the system of equations (1)–(8) are: the mass flow rate of air G kg/s at the outlet of the casing, which is removed from the rough grinding machine by the fan. In this case, the amount of air removed is determined depending on the diameter of the grinding wheel $d_{кр}$ according to the formula, m^3/h:

$$L_1 = 1{,}8 \cdot d_{кр}. \tag{15}$$

Formula (15) is valid for 250 mm<$d_{кр}$ <600 mm. The air velocity is determined from the formula:

$$u_i = \frac{G}{\rho \cdot S}, \tag{16}$$

where ρ — density, S — the area of the passage section.

The calculated speed of air intake in the intake opening of the casing is, m/s: $\upsilon_0 = 0{,}25 \cdot \upsilon_{окр}$ — from the circumferential speed when the plume is directed into the intake opening of the suction duct; $\upsilon_0 = (0{,}3...0{,}4) \cdot \upsilon_{окр}$ — when the dust plume is directed parallel to the suction opening of the connected air duct.

The circumferential speed of the grinding wheel is determined by the formula:

$$\upsilon_{кр} = \frac{\pi \cdot d_{кр} \cdot n}{60 \cdot 1000}, \tag{17}$$

where n — the speed of rotation of the grinding wheel, taken from the technical characteristics of the machine.

Figures 3a, b show the geometry and design scheme of the studied shaped shelter of the rough grinding machine.

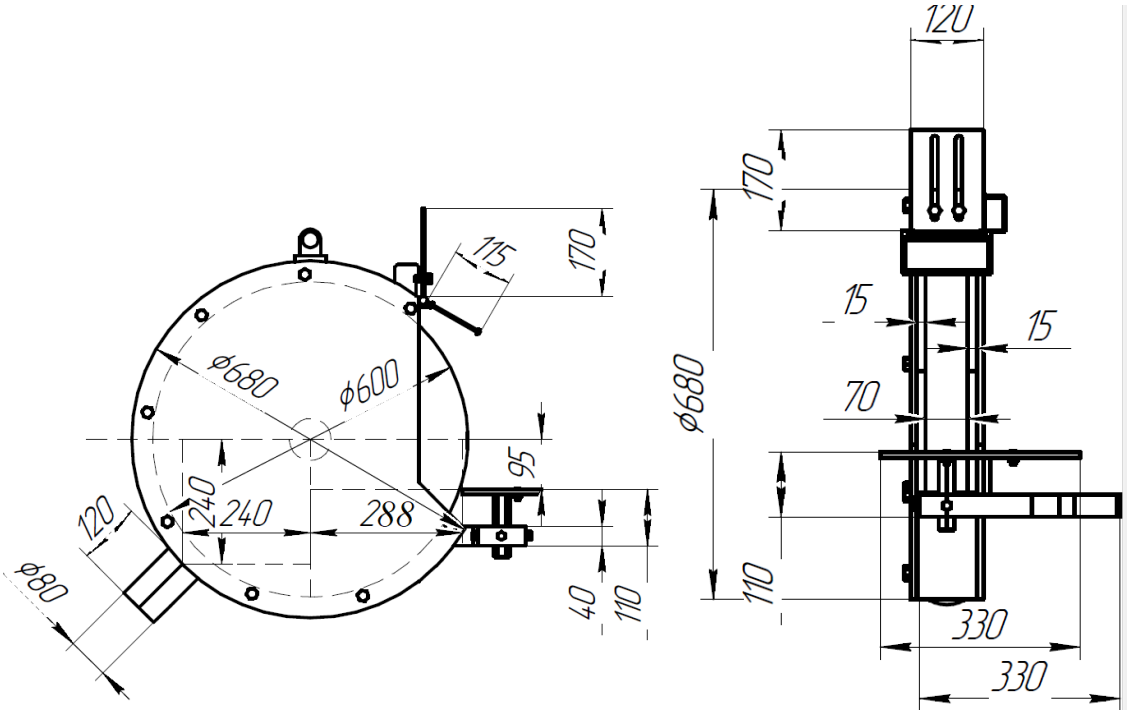

a) *b*)

Fig. 3. Basic design scheme: a — side view, b — end view

Problem Statement. Computer model of a rough grinding machine aspiration.

A 3D model of the area was created, starting from the air inlet (the point of contact of the wheel with the part — the formation of abrasive) to the middle of the grinding wheel. The 3D model simulates an internal air domain bounded by a circle, a casing, and free surfaces (air inlets and outlets) (Fig. 4a, b).

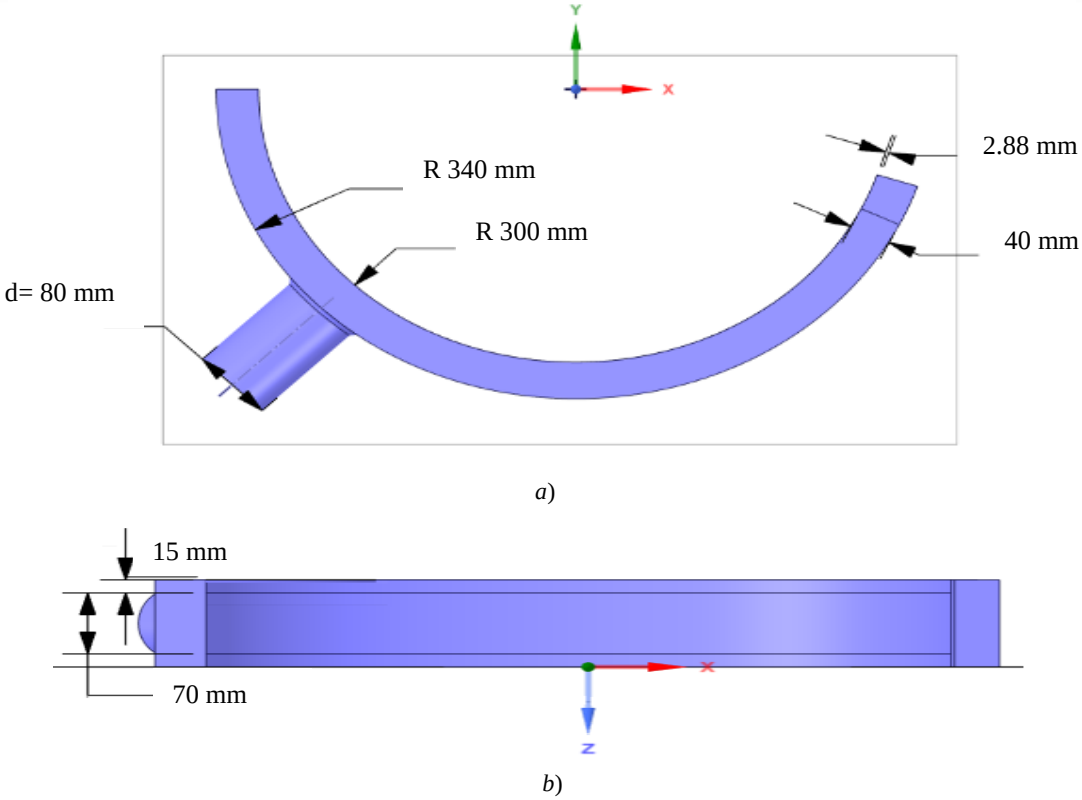

Fig. 4. Computational domain: a — side view, b — top view

The gap between the outer surface of the grinding wheel and the inner surface of the protective casing is assumed to be 40 mm in the first approximation.

This design parameter of the machine can be changed. A 5 mm chamfer has been added to the inlet.

Boundary conditions:

1. Wall, sticking conditions (zero speeds). On this surface, the air moves at the speed of rotation of the wheel (Table 2).

2. The inlet of the air flow at a speed of 30.77 m/s.

3. Suction, air flow rate of 1080 m^3/h (Fig. 5 a).

4. Free surfaces with zero pressure relative to the external atmospheric pressure. Air can enter and exit through these surfaces, depending on the task parameters. The gap between the grinding wheel and the casing is also a free surface that can be changed (Fig. 5 b).

Table 2

Calculated parameters

Name	Value	Unit of measurement
Air density	1,225	kg/m^3
Air viscosity	1,7894·10^{-5}	kg/m·s
Wheel speed	980	rpm

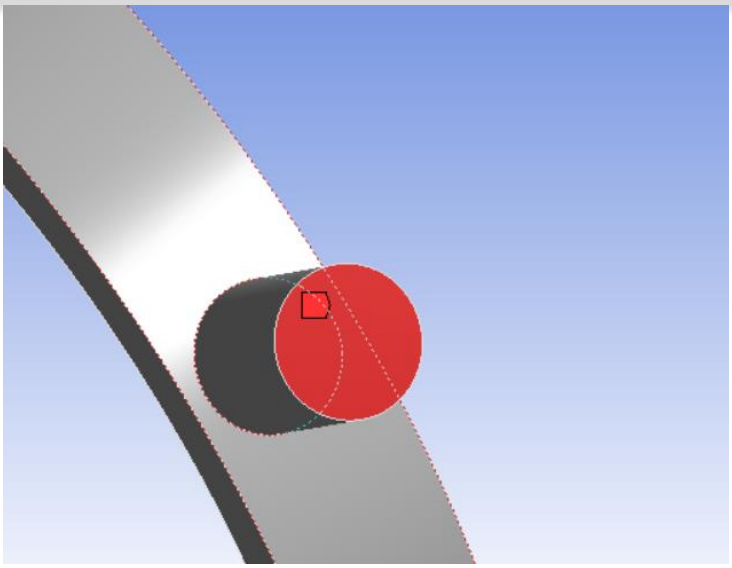

a)

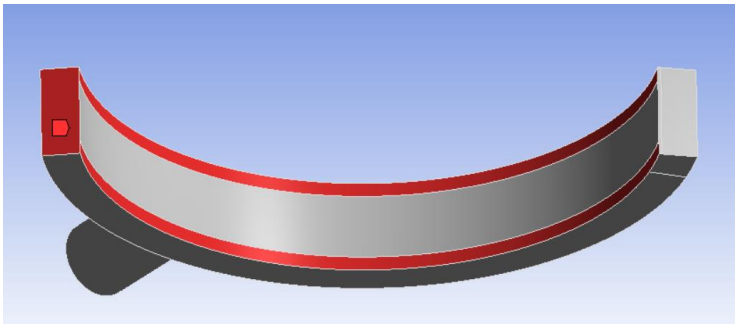

b)

Fig. 5. Boundary conditions in the model: a — suction from the machine, air flow of 1080 m^3/h, b — free surfaces with zero pressure

Calculated grid of finite volumes. Model calculations of the processes were carried out with different grid structures. The size of the calculated grid in the middle zones of the channels is 25 mm. Above the outer borders and in the transition area from the casing to the suction pipe, thickening in the form of wall layers is performed (Fig. 6a, b).

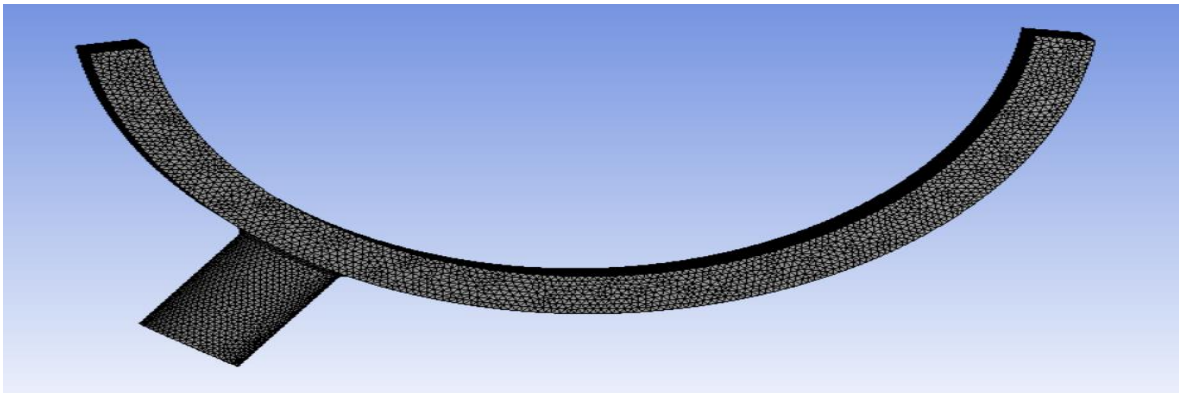

a)

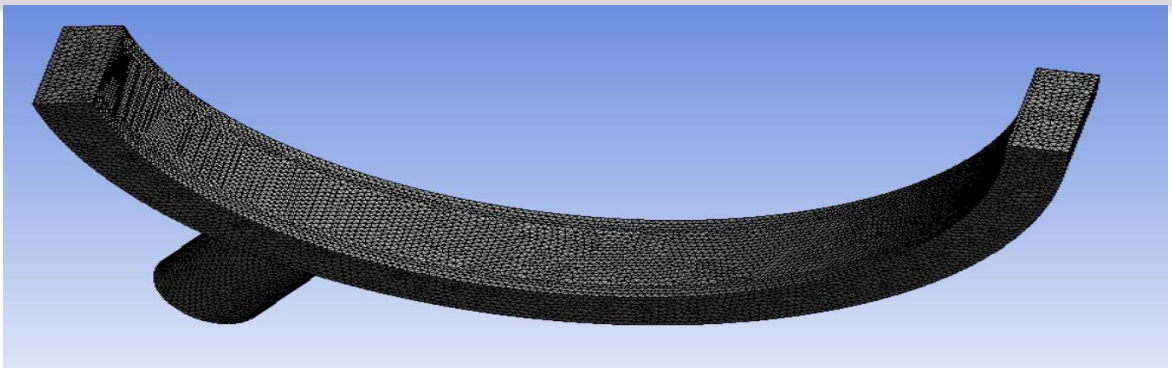

b)

Fig. 6. Grid of finite volumes: a — side view, b — top view

In the 3D model, the corresponding boundaries that are responsible for the boundary conditions of the model are highlighted in red (Fig. 5, 7).

The section in Fig. 7 models the support for the parts. For convenience, the support surface is located along the radius. The surface of the stand in the boundary conditions is the boundary conditions of the wall, the area between the table and the wheel is the air inlet at the appropriate speed, and the part not covered by the casing is the free surface for the air inlet and outlet (marked in green).

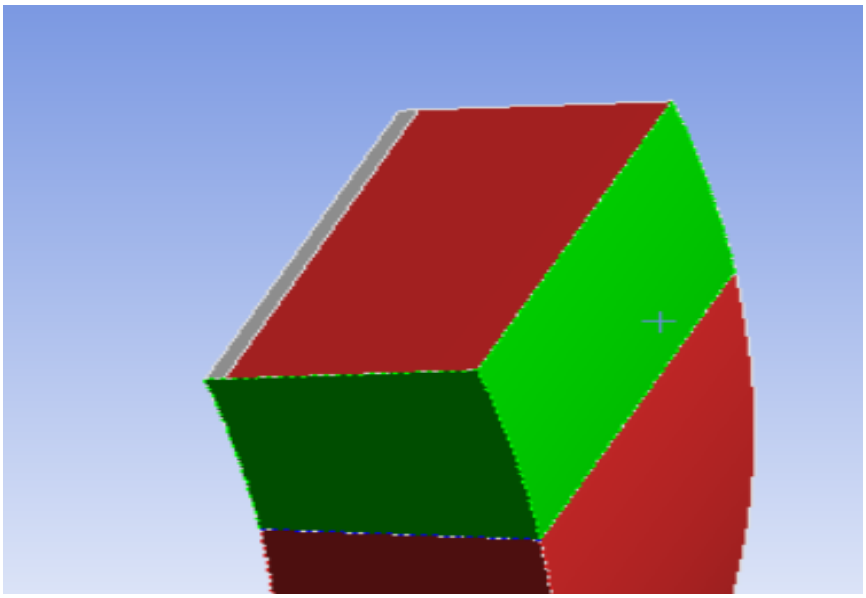

Fig. 7. Model of the support

Results of model calculations of shelter aerodynamics. Figure 8 shows the flow velocity field formed during the operation of the hood of the rough grinding machine. As you can see from the calculation results, the field is extremely uneven. The speeds vary from a maximum of 60-80 m/s at the inlet of the flows into the suction pipe of the machine to a minimum in the space of the channel between the grinding wheel and the casing [14]. For a more detailed understanding of the flow velocity distribution pattern, we will construct the current velocity lines (Fig. 9–12).

Figure 9 shows the results of the modeling of the flow motion in the space between the abrasive wheel and the casing, as well as in the cylindrical branch pipe of the suction hood.

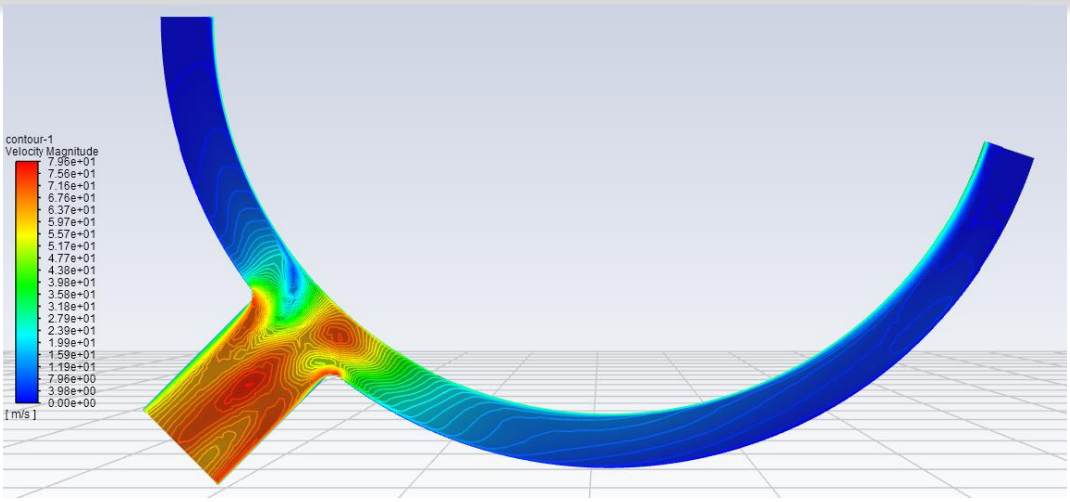

Fig. 8. Flow velocity field in the channel

Figure 9 shows the velocity current lines — the trajectories of particle motion. The color is responsible for the trajectories numbers. It can be seen that the input velocity of the air flow into the closed part of the machine casing corresponds to the values of 30-34 m/s. At a distance from the exhaust pipe, on the contrary, a reverse air flow with low speeds is formed.

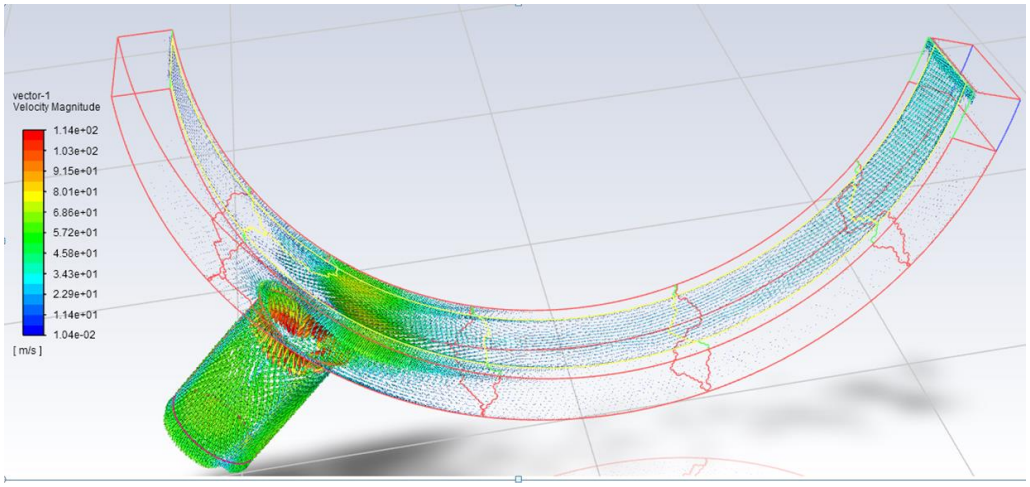

Fig. 9. Image of flow velocity vectors

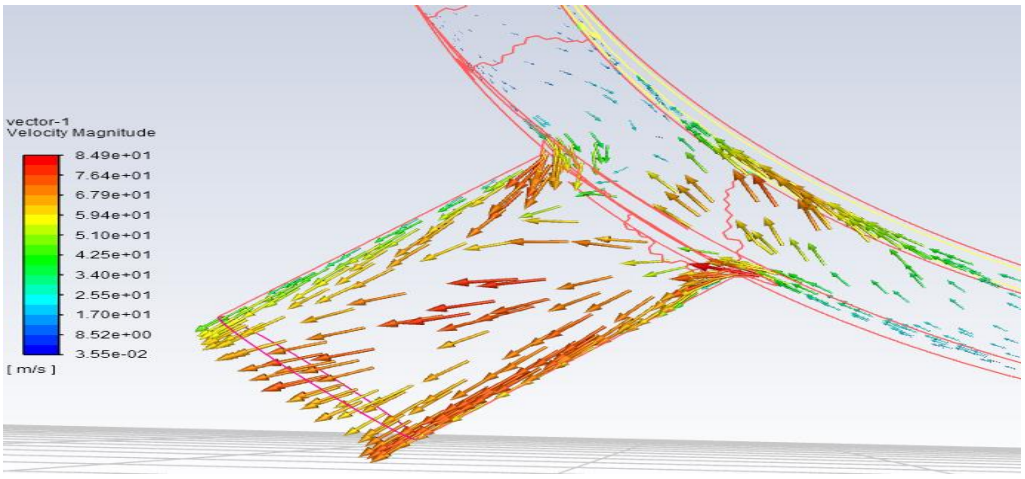

Fig. 10. Numerical values of flow velocity vectors

Velocity current lines are the trajectories of the expected dust particles. The color is responsible for the trajectories numbering.

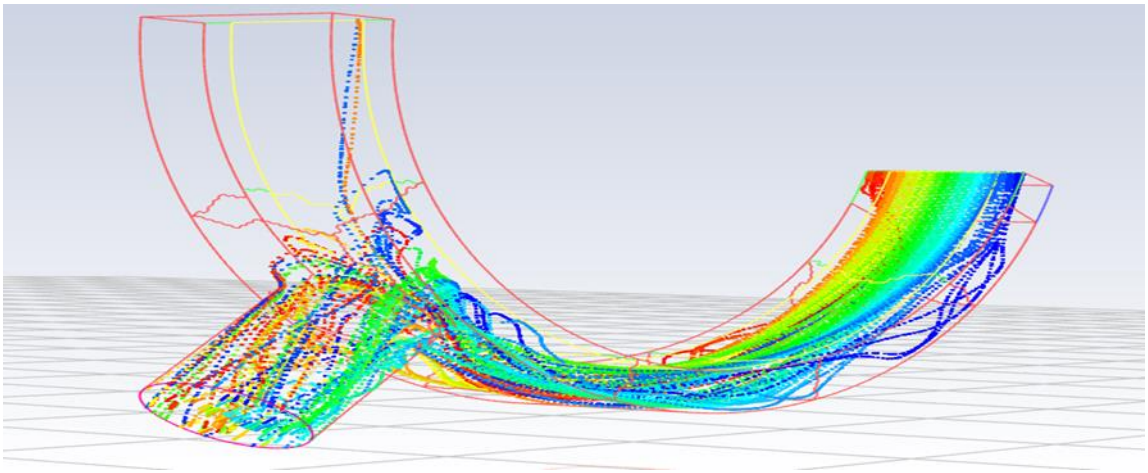

Fig. 11. Image of current velocity lines

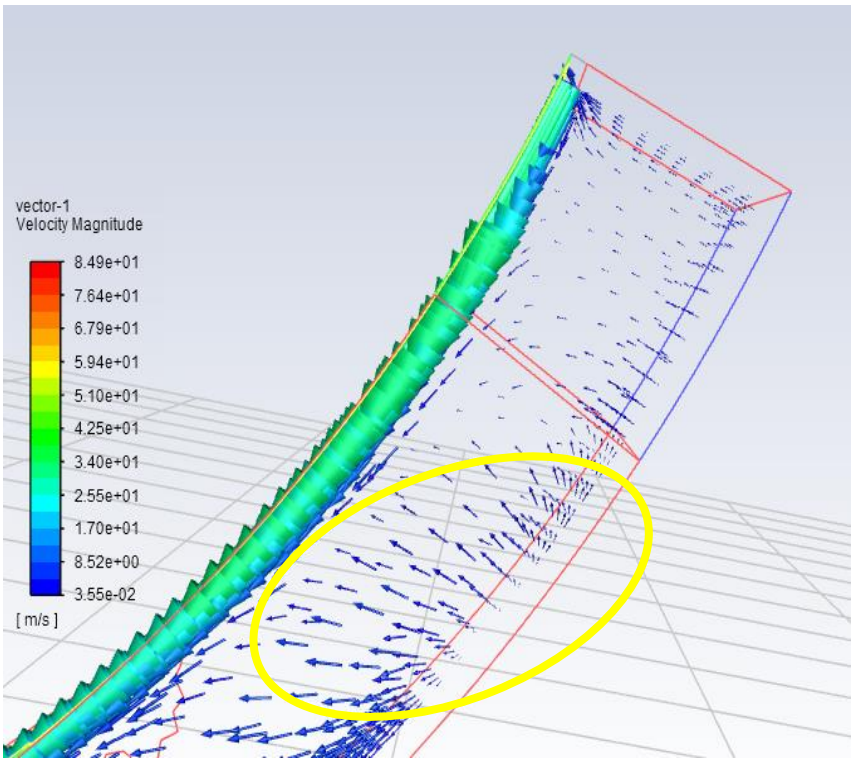

Fig. 12. Image of the vortices of the air flow at the entrance to the casing

The yellow outline shows the swirls at the beginning of the casing, where the flow divides in different directions from the casing wall.

According to the results of the CFD calculation, the average particle velocity at the suction site is about 60 m/s, but a more complex distribution pattern of the velocity gradient with local values up to 80 m/s is observed.

Figure 13 shows the flow velocity vectors at the outlet of the casing with the circular shape of the exhaust pipe.

It should be noted that in the immediate vicinity of the abrasive wheel, a reverse plume is formed, as in Figure 1, which leads to the release of dust particles to the operator's workplace. The speed of this flow is from 0.355 to 1.7 m/s (Fig. 13).

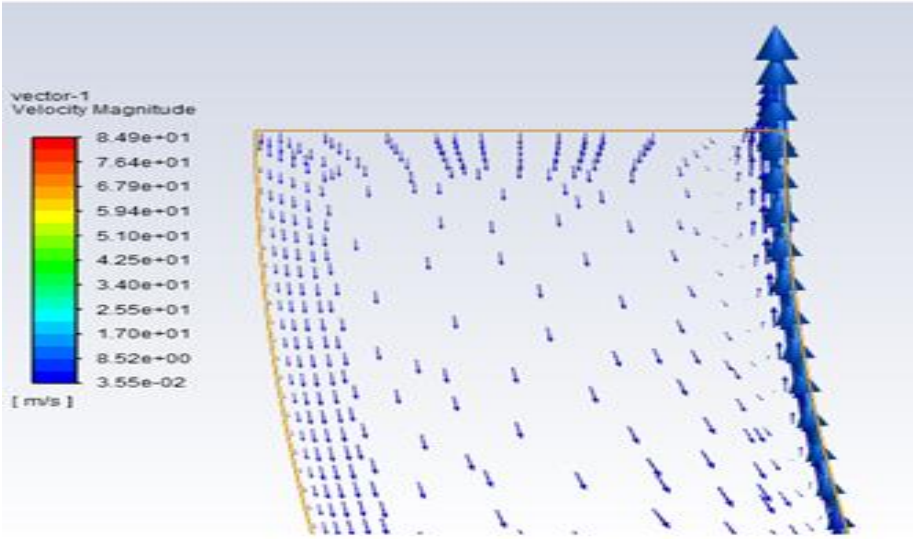

Fig. 13. Values of the velocity vectors of forward and reverse flows at the exit from the shelter

Conclusion. The developed computer model made it possible to determine the directional fields and the values of the air flow velocities in the closed area of the abrasive wheel and in the exhaust cylindrical pipe going to the fan.

However, to ascertain a more complete picture of dustiness of a grinder workplace you need to find out what are the field lines of the current flows and the values of velocity near the shaped shelter of the rough grinding machine, i.e. in the space where the circle is not closed by the shaped shelter.

The obtained fields and the values of the air flow velocities at the shaped shelter of the grinding machine (in the open part of the abrasive wheel), i.e. at the point where dust enters the air of the working area, will be further compared with the hovering velocities of various dust particles, which will ultimately determine the efficiency of their capture.

Conclusions:

1. Mathematical and computer models of aspiration of a rough grinding machine are developed, implemented in the modern software Apsus.

2. The computer model allows you to determine the rational (minimum necessary) amount of air removed and the effect of abrasive wear of the grinding wheel on the aerodynamic characteristics of the shelter of the grinding machine.

3. The dependences are obtained describing the velocity fields of the flow in a closed region of the abrasive wheel, influencing the formation of lines of current flow near the shaped shelter of the rough grinding machine, which in the future will allow us to determine the shelter effectiveness of the rough grinding machine, including at the design stage.

References

1. Kugultinov S. D., Kovalchuk A. K., Portnov I. I. Tekhnologiya obrabotki konstruktsionnykh materialov. 3-e izd., pererab. i dop. [Technology of processing of structural materials. 3rd ed., reprint. and add.]. Moscow: Bauman Moscow State Technical University Publishing house. 2010. p. 268–270 (In Russ.).

2. Pasyutina O. V. Bezopasnost' truda i pozharnaya bezopasnost' pri mekhanicheskoy obrabotke metalla na stankakh i liniyakh [Occupational safety and fire safety in metal machining on machines and lines]. Minsk: RIPO. 2012. 108 p. (In Russ.).

3. Zalaeva S. Sh., Nosatova E. A., Rybka O. A. Proizvodstvennaya sanitariya i gigiena truda: uch. posobie v 3 ch. Ch. 2. Vrednye veshchestva. Proizvodstvennyy shum [Industrial sanitation and occupational hygiene: study guide in 3 parts. Part 2. Harmful substances. Production noise]. Belgorod: BGTU Publishing house, 2008. p. 93. (In Russ.).

4. Bykov L. V., Molchanov A. M., Yanyshev D. S. Osnovy vychislitel'nogo teploobmena i gidrodinamiki [Fundamentals of computational heat transfer and hydrodynamics]. Moscow: URSS, 2019. p. 124. (In Russ.).

5. Snegirev A. Yu. Vysokoproizvoditel'nye vychisleniya v tekhnicheskoy fizike. Chislennoe modelirovanie turbulentnykh techeniy: ucheb. posobie [High-performance computing in technical physics. Numerical simulation of turbulent flows: textbook]. Sankt-Petersburg: Publishing house of Polytechnic University 2009. 143 p. (In Russ.).

6. Yang T.S., Shy S.S., 2005. Two-way interaction between solid particles and homogeneous air turbulence: particle settling rate and turbulence modification measurements. J. Fluid Mech;526:171–216. DOI : https://doi.org/10.1017/S0022112004002861

7. Weigang Yao, Meng Liou A nonlinear modeling approach using weighted piecewise series and its applications to predict unsteady flows. Journal of Computational Physics. 2016;318:58-81. DOI : https://doi.org/10.1016/j.jcp.2016.04.052

8. Matyushenko A. A., Garbaruk A. V., Adjustment of the k-ω SST turbulence model for prediction of airfoil characteristics near stall. Journal of Physics: Conference Series., 18th International Conference Physic A. SPb. 2016;769:1–7. DOI : https://doi.org/10.1088/1742-6596/769/1/012082

9. Yoshizawa A., Nisizima S., Shimomura Y., Kobayashi H., Matsuo Y., Abe H., Fujiwara H., A new methodology for Reynolds-averaged modeling based on the amalgamation of heuristic-modeling and turbulence-theory methods. Journal of Fluids Engineering. 2006;18(3) DOI : https://doi.org/10.1063/1.2186669

10. Walters D. K., Cokljat D. A Three-Equation Eddy-Viscosity Model for Reynolds-Averaged Navier-Stokes Simulations of Transitional Flows. Journal of Fluids Engineering. 2008;130(12):14 DOI : https://doi.org/10.1115/1.2979230

11. Hamlington P. E., Schumacher J., Dahm W. J. A. Local and nonlocal strain rate fields and vorticity alignment in turbulent flows. Journal Physics of Fluids. 2008;7(2) DOI : https://doi.org/10.1103/PhysRevE.77.026303

12. Menter F. R., Egorov Y. The Scale-Adaptive Simulation Method for Unsteady Turbulent Flow Predictions. Pt. 1: Theory and Model Description. Journal Flow Turbulence and Combustion. 2010;85:113–138. DOI : https://doi.org/10.1007/s10494-010-9264-5

13. Bulygin Yu. I., Shchekina E. V., Maslenskiy V. V. Razrabotka elementov sistemy normalizatsii mikroklimata v kabine zernouborochnogo kombaina Torum [Development of microclimate normalization system elements in the cabin of Torum grain harvester]. Safety of Technogenic and Natural Systems. 2019;2:2–12. (In Russ.). DOI : https://doi.org/10.23947/2541-9129-2019-2-2-12

14. Bulygin Yu. I., Azimova N. N., Kuptsova I. S. Problemy proektirovaniya pyleochistnogo oborudovaniya v promyshlennosti [Problems of designing dust cleaning equipment in the industry]. Safety of Technogenic and Natural Systems 2018;1–2:2–12. (In Russ.). DOI : https://doi.org/10.23947/2541-9129-2018-1-2-2-12

Submitted 23.12.2020
Scheduled in the issue 27.01.2021

Author:

Kuptsova, Irina S., Junior Researcher, Center for Scientific Competencies, Don State Technical University (1, Gagarin sq., Rostov-on-Don, RF, 344003), ORCID: http://orcid.org/0000-0003-2236-0384, i-kyptsova@mail.ru